Statistics of LES Simulations of Large Wind Farms.

Søren Juhl Andersen[1a]**, Jens Nørkær Sørensen**[1]**, Robert Mikkelsen**[1]**, and Stefan Ivanell**[2]

[1] DTU Wind Energy, Technical University of Denmark, 2800 Lyngby, Denmark
[2] Uppsala University, Dep. of Earth Sciences, Campus Gotland, Visby, Sweden.

E-mail: [a]`sjan@dtu.dk`

Abstract. Numerous large eddy simulations are performed of large wind farms using the actuator line method, which has been fully coupled to the aero-elastic code, Flex5. The higher order moments of the flow field inside large wind farms is examined in order to determine a representative reference velocity. The statistical moments appear to collapse and hence the turbulence inside large wind farms can potentially be scaled accordingly. The thrust coefficient is estimated by two different reference velocities and the generic C_T expression by Frandsen. A reference velocity derived from the power production is shown to give very good agreement and furthermore enables the very good estimation of the thrust force using only the steady C_T-curve, even for very short time samples. Finally, the effective turbulence inside large wind farms and the equivalent loads are examined.

1. Introduction

Wind farms continues to increase in size and consequently approach the asymptotic state or infinite wind farm scenario, where there is balance between the energy entrainment and the energy extracted by the turbines, e.g. Calaf et al. [1]. The balance has recently been exploited by Stevens et al. [2] to combine a simple engineering wake model with a boundary layer model based on momentum theory to yield a good approximations for mean power production for various turbine spacings.

However, Andersen et al. [3] compared several large eddy simulations(LES) of large wind farms conducted by several different institutes and found comparable, yet significant temporal variability inside large farms due to the highly dynamic and turbulent flow. The variability is inherent to LES and either requires relative long averaging time or enables the analysis of higher order statistics, *e.g.* examine the probability density distributions of the various parameters.

The short time variability related to the turbulent fluctuations govern the loads on the turbines. These loads are increase in wake situation in large wind farms, *e.g.* Larsen et al. [4].

State-of-the-art numerical flow and aero-elastic modeling is combined to assess both variability in the turbulent wind field as well as get the instantaneous loads and performance of the turbines.

2. Methodology

2.1. Numerical Implementation

The large wind farms are modeled using EllipSys3D, which solves the discretized incompressible Navier-Stokes equations using a finite volume approach in general curvilinear coordinates.

EllipSys3D is formulated in pressure-velocity variables, where the pressure correction equation is solved by the PISO algorithm and the Rhie-Chow interpolation technique is used to avoid pressure decoupling. The convective terms are discretized using a combination of the third order QUICK scheme and the fourth order CDS scheme in order to avoid numerical wiggles. EllipSys3D is develop at DTU, see Michelsen [5]) and Risø(Sørensen[6]).

Several wind farms are modeled with Large Eddy Simulations (LES) and the actuator line(AL) method, see Sørensen and Shen [7]. AL applies body forces along rotating lines, which represents the turbine blades. The imposed body forces are calculated using Flex5, which is an aero-elastic code used to calculate loads and deflections of wind turbines, see e.g. Øye [8].

The actuator line are fully coupled to Flex5, which means that the turbines are responding directly to the turbulent inflow with deflections and that the turbine controller is active, see Sørensen et al. [9] for details.

The atmospheric boundary layer(ABL) is prescribed explicitly by imposing additional body forces in the flow as described by Troldborg et al. [11], who showed that the effective magnitude of the body forces are inversely proportional to the Reynolds number and there insignificant.

The present yields a prescribed boundary layer as a combination of a parabolic and a power law profile governed by:

$$U_{pbl}(z) = \begin{cases} U_0 \cdot (c_2 z^2 + c_1 z) & z \leq \Delta_{PBL} \\ U_0 \cdot \left(\frac{z}{H_{hub}}\right)^{\alpha_{PBL}} & z > \Delta_{PBL} \end{cases}$$

where Δ_{PBL} determines the height, where the profile shift from the parabolic to power law profile. H_{hub} is the hub height, c_1, c_2, and α_{PBL} are shape parameters. c_1 and c_2 are calculated to ensure a smooth transition between the parabolic and the power law expression.

Finally, atmospheric turbulence is also added by body forces in a plane upstream the turbine. The body forces are derived based on stochastically generated turbulence using the Mann model, see Mann [12] and [13].

Hence, the filtered flow field is determined by solving the 3D incompressible Navier-Stokes equations with added body forces, **f**:

$$\frac{\partial \mathbf{V}}{\partial t} + \mathbf{V} \cdot \nabla \mathbf{V} = -\frac{1}{\rho}\nabla p + \nu \nabla^2 \mathbf{V} + \mathbf{f}. \ \ \nabla \cdot \mathbf{V} = 0 \tag{1}$$

using Large Eddy Simulation. The sub-grid scale (SGS) viscosity used in the LES is modeled using the vorticity based mixing scale by Ta Phuoc et al. [14].

2.2. Turbine
The modeled turbine is an upscaled version of the NM80 turbine, which is proprietary to Vestas Wind Systems A/S, see Madsen et al. [15]. NM80 has a radius $R = 40m$ and is rated to $2.75MW$ for $U_{hub} = 14$m/s.

The turbine has an active controller, which is a combination of a variable speed P-controller for small wind speeds($U_{hub} < 14m/s$) and a PI-pitch angle controller for higher wind speeds. The implemented controller essentially means that the rotor is not constantly loaded, and as such it operates like a real turbine.

2.3. Simulations Overview
A total of eight large wind farms have been modeled, which each include 16 turbines in the streamwise direction and with cyclic boundary conditions in the lateral to mimic infinitely wide farms. The main parameters are streamwise and lateral spacings(S_X, S_Y), turbulence intensity(TI) and freestream velocity at hub height(U_0). The simulations have been run for two flow throughs to flush the domain of any transients and continued $60mins$ afterwards. Aero-elastic output is saved every $0.1s$. The parameters are summarized in Table 1.

Table 1. Overview of simulations

Name	U_0	TI	Shear	Spacing/Domain ($S_X \times S_Y$)	Time
A	$8m/s$	0%	0.14	$12R \times 20R$	$16WT \times 60min$
B	$8m/s$	3%	0.14	$12R \times 20R$	$16WT \times 60min$
C	$8m/s$	15%	0.14	$12R \times 20R$	$16WT \times 60min$
D	$15m/s$	15%	0.14	$12R \times 20R$	$16WT \times 60min$
E	$8m/s$	0%	0.14	$12R \times 12R$	$16WT \times 60min$
F	$15m/s$	0%	0.14	$12R \times 12R$	$16WT \times 60min$
G	$8m/s$	0%	0.14	$14R \times 14R$	$16WT \times 60min$
H	$8m/s$	0%	0.14	$20R \times 20R$	$16WT \times 60min$

3. Results

3.1. Statistical Moments

Basic statistics(*e.g.* mean and standard deviation) of the LES resolved turbulence inside wind farms show significant variability as previously discussed by Andersen et al. [3], and hence require long simulation periods or higher order statistics. Figure 1 shows the development in mean, standard deviation, skewness, and kurtosis of the normalized velocity($\frac{U_{hub}}{U_0}$) at hub height for each of the eight simulations. The first four simulations($A-D$) are emphasized in brighter colors to show the effect of atmospheric turbulence. Clearly, the statistics converge by the fifth or sixth turbine. The means and standard deviations show the expected development through the farm with some variation in the final converged level, which is particular related to atmospheric turbulence. The vertical axes in Figure 1(c)-(e) have been limited for clarity. The large values arise due to the absence of atmospheric turbulence, so the statistics are for skewed for the first turbines untill the wakes break down into proper small scale turbulence.

However, the dependence on atmospheric turbulence disappears, when the statistical moments are normalized using the local mean velocity rather than the freestream, see Figure 1(c).

The skewness and kurtosis appears to converge towards approximately the same levels for all the different farm setups. There is a minor difference due to atmospheric turbulence as it yields slightly negative skewness, whereas the inherent farm turbulence yields slightly positive skewness, but it would indicate that the farm turbulence is to some degree scalable. The values of kurtosis is very close to 3 corresponding to a Gaussian distribution, although slightly positively skewed. A Gaussian distribution is often assumed by stochastic turbulence models, see the recent study by Berg et al. [16], who found only a minor influence of Gaussian or non-Gaussian velocity distribution on the equivalent loads.

3.2. Reference Velocity and Thrust in Large Farms

The previous analysis clearly highlights the importance of determining the appropriate reference velocity for flow inside large wind farms. The reference velocity is a typical issue when assessing the thrust coefficient $C_T = \frac{T}{\frac{1}{2}\rho A U_{ref}^2}$ inside large wind farms. The reference velocity is usually the freestream velocity, but the freestream velocity is far upstream and no longer representative for a turbine inside a farm. Frandsen [17] derived a generic expression for the thrust coefficient based on the velocity at hub height given by $C_T = \frac{7}{U_{hub}}$ and Calaf et al. [1] derived an expression for a farm C_T based on induction factor as well as time and rotor averaged velocity. The actual thrust force is known directly from the fully coupled simulations, so the generic expression as well as two different velocities are examined and validated against the computed thrust. Two different velocities are examined:

- U_{hub}: Velocity at hub height, here extracted 1R upstream.
- U_*: A rotor averaged velocity is derived from the steady power curve and taking power as a proxy for the velocity. This approach is often utilized for measurement data, e.g. SCADA.
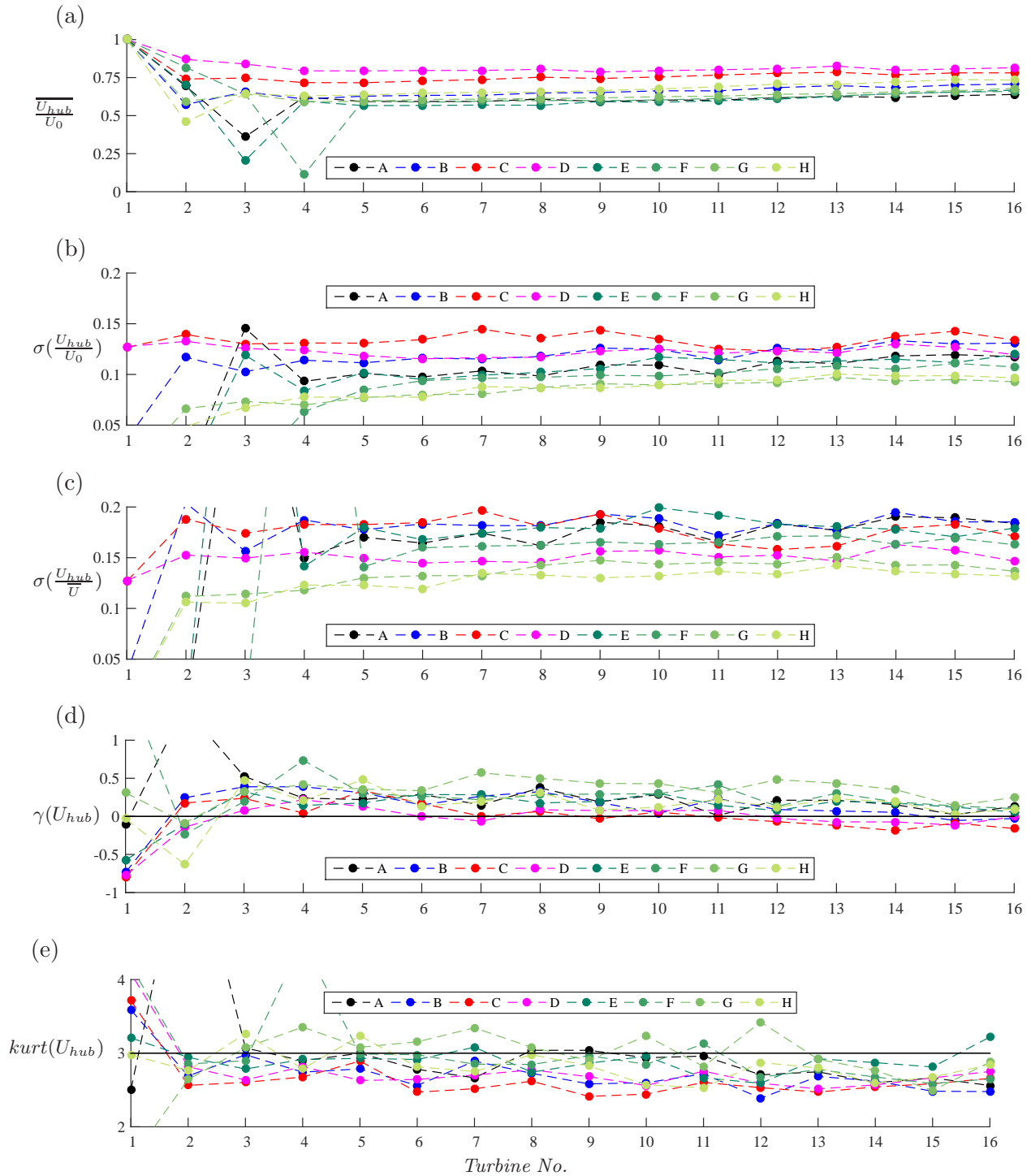
Figure 1. Statistics of the velocity at hub height in numerous large wind farms simulations. (a) Mean, (b) standard deviation, (c) standard deviation based on local mean velocity((a)), (d) skewness, and (e) kurtorsis. Black line corresponds to a normal distribution.

The steady performance curves(*e.g.* power coefficient C_P, power P, thrust T, and C_T) has been derived from aero-elastic simulations with uniform inflow for all wind speeds.

Figure 2 shows the performance data of the 6th-16th turbine in all the simulations for three different temporal windows, *i.e.* running mean has been taken of the operational data over windows of $1s$, $60s$, and $600s$. Hence, the performance data from the eight simulations constitute a total of 88 hours of operational data. The black lines yield the steady performance curves. The power production compared to the power curve based on the velocity at hub height is shown in blue points((a)-(c)). The blue points follow the trends of the steady state power curve, but with a significant spread. The spread clearly decrease as the statistical window is increased, but the resulting power curve is higher than the steady power curve due to turbulence. The red points correspond to the rotor averaged velocity based on the power production denoted U_*.

Figure 2(d)-(f) shows the different thrust and power realizations from the eight simulations for different temporal windows compared to the steady $T - P$-curve. Despite very large variability in the simulations, the figure shows how the turbine is operating as expected and how there is a direct correlation between power and thrust for below rated.
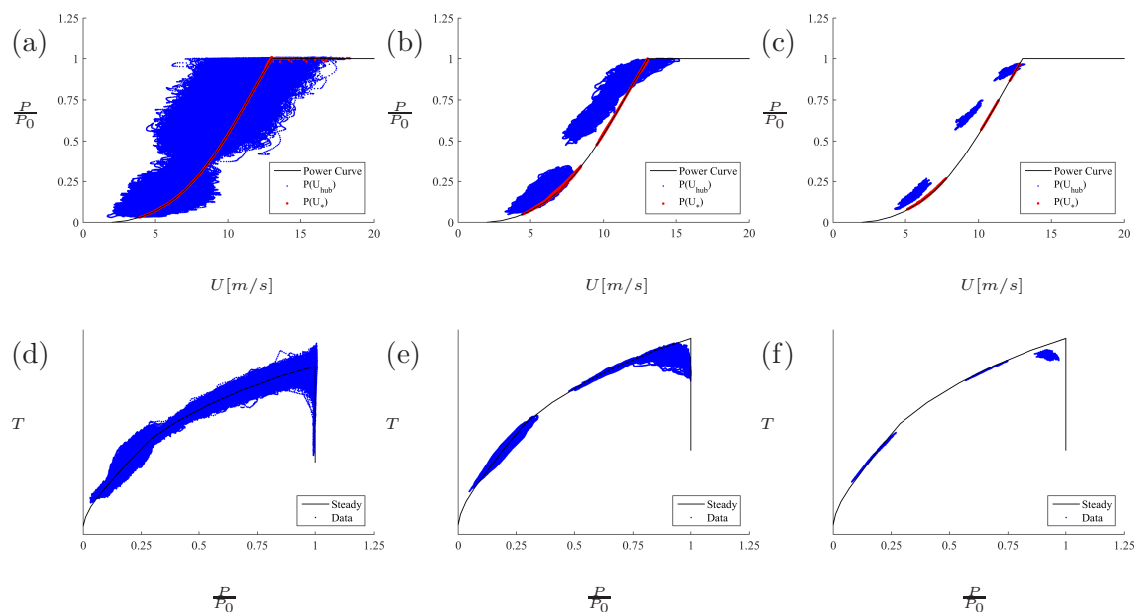

Figure 2. Performance data for power((a)-(c)) and thrust((d)-(f)) with averaging windows of $1s$, $60s$, and $600s$, respectively.

Figure 3 shows a comparison of the steady C_T-C_P-curve compared to the three estimated C_T using U_{hub}(blue), U_*(red), and the generic expression by Frandsen(green). Clearly, estimating C_T based on U_{hub} yields very big spread and the comparison is very poor, *i.e.* the reference velocity is wrong as the C_P-values clearly exceeds any sensible range. Frandsen yield a good comparison, particular for averaged velocities, but with a significant spread for the short sampling times. C_T and C_P based on the rotor averaged velocity U_* shows a very good agreement with the steady C_T-C_P-curve for both short and long sampling times, hence indicating that U_* is an appropriate reference velocity. It should be noted also how the discrepancy for large C_T for both Frandsen and U_*, *i.e.* the vertical rise of samples for high C_P is presumably related to the Glauert correction, which is invalid for low velocities.

Hence, the turbine thrust can be estimated using only the power production and steady C_T-curve(not shown for brevity). The average cross-correlation of the estimated thrust and the actual thrust force from the 11 considered turbines in the fully coupled simulations is compared in Table 2. Clearly, the power is a very good proxy for determining a representative reference
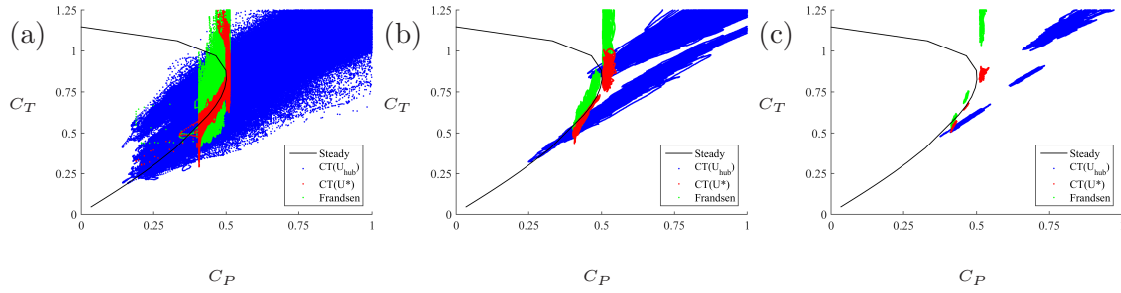
Figure 3. Performance data based on velocity at hub height and power derived velocity compared to steady C_T-C_P-curves for averaging windows of $1s$, $60s$, and $600s$, respectively. Generic expression of Frandsen included.

velocity, which gives the correct thrust force. The correlation is very high for both short and long sampling times. It is perhaps surprising with a high correlation for short temporal window as the the influence of the controller does not alter the correlation for the $1s$ samples. However, simulation D has a significant lower correlation due to a freestream velocity above rated and high atmospheric turbulence. Simulation F also has an initial freestream velocity above rated, but effective wind speed inside the farm is significantly lower than in Simulation D due to the decreased lateral spacing and particular the absence of atmospheric turbulence to increase energy entrainment. Hence, for Simulation D, the turbines are operating in the most dynamic control regime, which is not captured by this simple approach and would include the pitch dependency. An attempt was made to include the pitch, but it did not initially yield satisfactory results as the turbine operation effectively occurs along two distinct lines and the turbines are in and out of above rated conditions. It could presumably be more successful for situations significantly above rated, where power production is maintained at rated.

Table 2. Average cross-correlation of the assessed thrust and actual thrust from the fully coupled simulations. Average based on 11 turbine time series for each simulation.

Name	$T_{win} = 1s$	$T_{win} = 60s$	$T_{win} = 600s$
A	0.94	0.99	0.99
B	0.97	0.99	1.00
C	0.97	1.00	0.99
D	−	0.28	0.45
E	0.94	0.99	0.99
F	0.95	0.99	0.99
G	0.96	0.99	1.00
H	0.96	0.99	0.99

Similarly, the rotor averaged fluctuations can be assessed from the instantaneous power signal and converted to U'_*. Figure 4 show the standard deviations of U'_{hub} vs U'_* for different averaging windows. Power is an integrated quantity and the extend of the rotor acts as spatial filter, so generally the rotor averaged fluctuations are less than the fluctuations as expected, and for longer samples the statistics are correlated.

The turbulent fluctuations directly affect the loads acting on the turbine, so determining an effective farm turbulence is important. Frandsen [17] derived an expression for the effective farm turbulence as the sum of squares of the atmospheric turbulence(TI_0) and the turbulence added by the presence of the turbines($TI_{add,wf}$):

$$TI^2_{wf} = TI^2_0 + TI^2_{add,wf}, \quad \text{where} \quad TI^2_{add,wf} \approx \frac{0.36}{1 + 0.2\sqrt{\frac{S_X S_Y}{C_T}}} \tag{2}$$
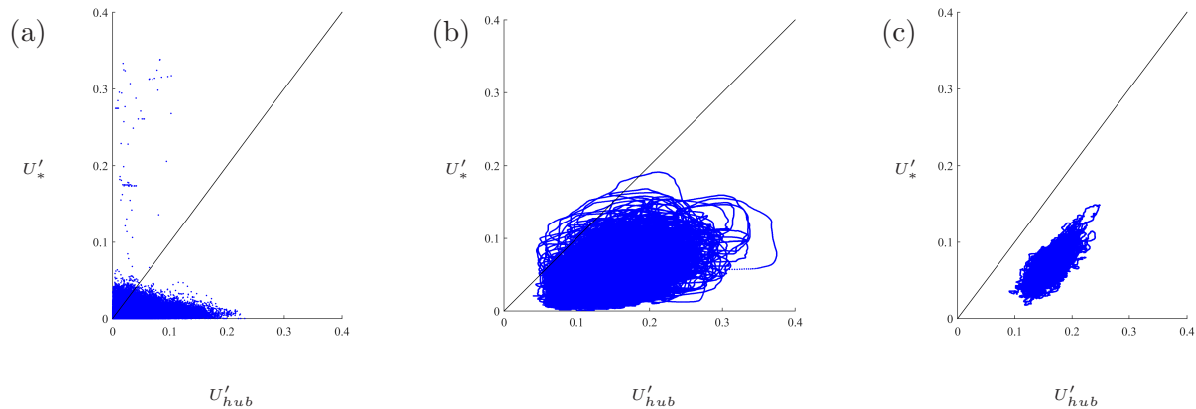
Figure 4. Correlation between velocity fluctuations at hub height(U'_{hub}) and derived from the power fluctuations(U'_*) for averaging windows of $1s$, $60s$, and $600s$, respectively.

where CT of the first turbine, *i.e.* relative to the freestream velocity is used. Figure 5 compares the farm turbulence calculated from Equation 3.2 and the turbulence at hub height from the LES simulations $A - D$. The added farm turbulence in the simulations are assessed as $TI_{add,LES} = TI^2_{wf} - TI^2_0$, since the turbulence inside the farm is known directly and corresponds to the total turbulence intensity based on all three velocity components:

$$TI_{wf} = \sqrt{1/3 \cdot \left(\frac{U'_{hub}}{U_0}^2 + \frac{V'_{hub}}{U_0}^2 + \frac{W'_{hub}}{U_0}^2 \right)} \qquad (3)$$

Equation 3.2 tends to overestimate the effective farm turbulence, which was expected by Frandsen. However, it is noteworthy that the estimated turbulence intensity is very good between the turbines, but that the induction or blockage from the turbine significantly reduces the turbulence intensity as it approaches the rotor.

The $10mins$ equivalent flapwise, tilting, and yaw moments are combined from the 6th-16th turbine for all the simulations to get full distributions and the equivalent moments are normalized by $\frac{1}{2}\rho A U_* U'_* R$ into an equivalent load coefficient based on both the reference average velocity and fluctuations, see Figure 6. The normalization scales the distributions to be overlapping and closer together. The presented normalization resulted in smaller spreads than $\frac{1}{2}\rho A U^2_* R$ and $\frac{1}{2}\rho A U'^2_* R$, and intuitively the loads depend on mean as well as fluctuating velocities. Simulation G yields higher loads and a significant longer tail, which could be related to the wake structures at this spacing, which would require additional investigation. However, the remaining simulations yields comparable distributions, although the simulations with high atmospheric turbulence are skewed.
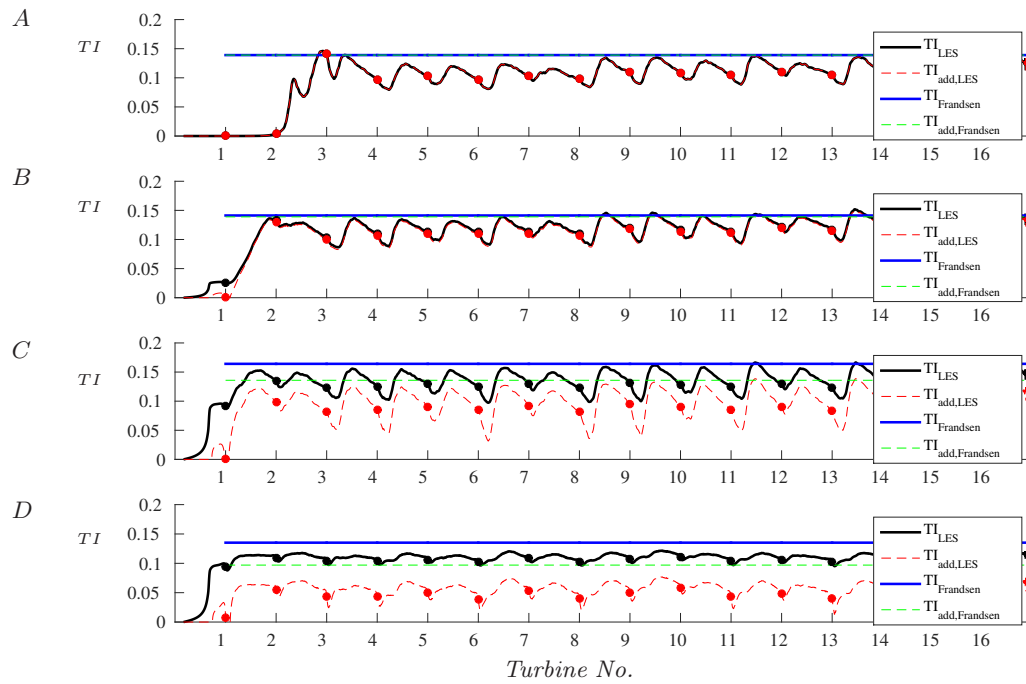
Figure 5. Added and effective farm turbulence estimates based on Frandsen and LES results from four simulations $A - D$. Turbine locations are marked by circles.
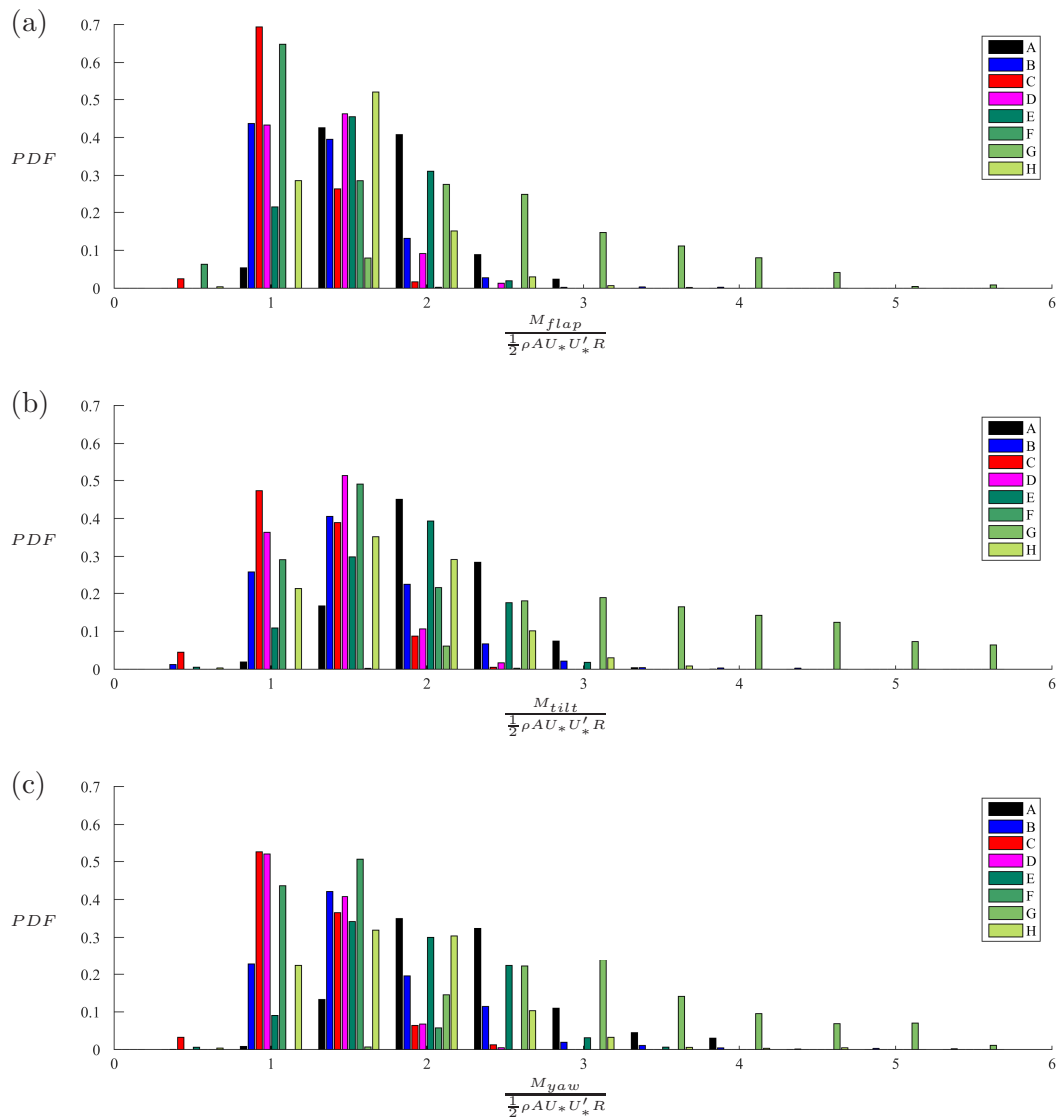
Figure 6. Normalised $10mins$ equivalent loads distributions for (a) flapwise moment, (b) tilting moment, and (c) yaw moment.

4. Conclusion and Discussion

A total of eight large wind farms have been modeled using LES and a fully aero-elastic implementation of the actuator line. Higher order statistics of the LES simulations are comparable and the influence of *e.g* atmospheric turbulence decrease, when scaled by a representative velocity. Determining a representative reference velocity will potentially enable scaling of farm turbulence across a range of farm parameters by the local mean and standard deviation.

A representative velocity derived from the steady power curve using the actual power production proved to be representative of the turbine performance in terms of C_T and enables the prediction of thrust force exerted by the turbine based only on the power production and steady C_T-curve to very high accuracy compared to the thrust calculated from the fully coupled LES simulations, except for the highly controlled regime around rated wind speed, which would require inclusion of the turbine pitch. This is shown to work for both long and short term samples, which is important when assessing thrust (coefficient) from measured SCADA data. The instantaneous thrust force can also be assessed from a power and C_T-curve and used in *e.g.* numerical simulations with actuator discs, which are not aero-elastically coupled and does not have a detailed turbine controller.

The standard expression for the effective farm turbulence is furthermore shown to be conservative, mainly since the induction from the turbine reduces the turbulence intensity. The equivalent load distributions for the flapwise, tilting, and yaw moments are furthermore are scaled to load coefficients by the reference velocity and fluctuations derived from the power production.

References

[1] Calaf M, Meneveau C and Meyers J 2010 *Physics of Fluids* **22** 1–16 ISSN 10706631, 10897666
[2] Stevens R J A M, Gayme D F and Meneveau C 2015 *Journal of Renewable and Sustainable Energy* **7** URL http://scitation.aip.org/content/aip/journal/jrse/7/2/10.1063/1.4915287
[3] Andersen S J, Witha B, Breton S P, Srensen J N, Mikkelsen R F and Ivanell S 2015 *Journal of Physics: Conference Series* **625** 012027 URL http://stacks.iop.org/1742-6596/625/i=1/a=012027
[4] Larsen T, Larsen G, Aagaard Madsen H, Thomsen K and Markilde Pedersen S 2015 URL http://orbit.dtu.dk/files/107150221/Comparison_of_measured_and_simulated_loads.pdf
[5] Michelsen J A 1992 Basis3D – a Platform for Development of Multiblock PDE Solvers Tech. rep. Danmarks Tekniske Universitet
[6] Sørensen N N 1995 *General Purpose Flow Solver Applied to Flow over Hills* Ph.D. thesis Technical University of Denmark
[7] Sørensen J N and Shen W Z 2002 *J. Fluids Eng.* **124** 393–399
[8] Øye S 11-12 April 1996 *Proceedings of 28th IEA Meeting of Experts Concerning State of the Art of Aeroelastic Codes for Wind Turbine Calculations. Available through International Energy Agency.* 71–76
[9] Sørensen J, Mikkelsen R, Henningson D, Ivanell S, Sarmast S and Andersen S 2015 *Phil. Trans. R. Soc. A* **373** ISSN 1364-503X
[10] Mikkelsen R, Sørensen J and Troldborg N 2007 *Prescribed wind shear modelling with the actuator line technique*
[11] Troldborg N, Sørensen J, Mikkelsen R and Sørensen N 2013 *Wind Energy* ISSN 1095-4244
[12] Mann J 1994 *Journal of Fluid Mechanics* **273** 141–168 ISSN 1469-7645
[13] Mann J 1998 *Probabilistic Engineering Mechanics* **13** 269–282 ISSN 0266-8920

[14] Ta Phuoc L, Lardat R, Coutanceau M and Pineau G 1994 Rechereche et analyse de modeles de turbulence de sous maille adaptes aux ecoulements instationnaires decolles.

[15] Aagaard Madsen H, Bak C, Schmidt Paulsen U, Gaunaa M, Fuglsang P, Romblad J, Olesen N, Enevoldsen P, Laursen J and Jensen L 2010 *The DAN-AERO MW Experiments* Denmark. Forskningscenter Risø. Risø-R (Danmarks Tekniske Universitet, Risø Nationallaboratoriet for Bæredygtig Energi)

[16] Berg J, Natarajan A, Mann J and Patton E 2016 *Wind Energy* ISSN 1095-4244 this project is sponsored by the Danish Energy Technology Development and Demonstration EUDP Project 64011-0352: Demonstration of a basis for tall wind turbine design. Partial support from the Danish Council for Strategic Research grant no. 09-067216 is also acknowledged

[17] Frandsen S 2007 *Turbulence and turbulence-generated structural loading in wind turbine clusters* Ph.D. thesis Denmark. Forskningscenter Risoe. Risoe-R risø-R-1188(EN)